

---

# Smart Polymeric Recognition of a Hexagonal Monolayer

B. LIEWEHR<sup>1,2</sup> and M. BACHMANN<sup>2</sup>

<sup>1</sup> *Institute of Physics, University of Rostock, Albert-Einstein-Straße 23, D-18059 Rostock, Germany*

<sup>2</sup> *Soft Matter Systems Research Group, Center for Simulational Physics, Department of Physics and Astronomy, University of Georgia, Athens, GA 30602, USA*

PACS 05.10.-a – Computational methods in statistical physics and nonlinear dynamics

PACS 68.43.-h – Chemisorption/physisorption: adsorbates on surfaces

PACS 82.35.Lr – Physical properties of polymers

**Abstract** – We investigate the adsorption of a flexible polymer at a hexagonally patterned monolayer. All conformational polymer phases are identified, which enables the construction of a hyperphase diagram, parameterized by temperature and monolayer adsorption strength. The energy scale associated with the adsorption strength is a material parameter of the hybrid system that generically accommodates the behavior of entire classes of polymers interacting with hexagonal substrates. We also discuss a bridge-building mechanism for the formation of unique layered polymer structures with potential for applications in nanoscale transport. High-quality data sets necessary for the statistical analysis of the structural phase behavior of the system were obtained in extensive generalized-ensemble Monte Carlo computer simulations.

**Introduction.** – Despite their huge structural phase space, flexible polymers have the impressive capability of undergoing distinct structural transitions. Most studied is the coil-globule or  $\Theta$  collapse transition that separates entropically dominant random, extended structures from the phase of globular conformations [1–3]. Globules, which are also long-range disordered, but compact and potentially ordered at short distances, are reminiscent of liquid droplets.

Much less understood is the crossover from these globules to ordered (such as crystalline or quasicrystalline icosahedral and decahedral) or disordered (amorphous) compact, solid phases. One reason is that features of this qualitative change in behavior are similar to first-order liquid-solid transitions. These are particularly difficult to study for finite systems because of significant surface effects. In meticulous studies, the relation between the structural characteristics, known from Lennard-Jones clusters of atoms [4–6], and the polymer chain length as well as temperature could be established for a coarse-grained model of finite flexible polymers [6–8].

In a different line of research, the adsorption properties of polymers at planar [9–12] and nonplanar [13–15] substrates have been of substantial interest, since hybrid organic-inorganic interfaces promise “smart material” properties with potential for nanosensory devices and other functional applications [16, 17].

The recent development of remarkable experimental techniques that made the exfoliation of atomic monolayers like graphene sheets possible created vibrant research fields in the materials sciences [18]. The detailed investigation of mechanical and electronic properties of individual, hexagonally structured atomic layers advanced the knowledge of properties of two-dimensional quasispherical and quasicylindrical atomic monolayer structures such as fullerenes and carbon nanotubes [19], respectively.

In this Letter, we combine these worlds and investigate the generic structural phases of a flexible, elastic polymer interacting with a hexagonal layer attached to a homogeneous substrate. Such a monolayer can be created by depositing or covalently binding atoms or small molecules to the underlying substrate. Flexible polymers can more easily adapt to their environment than other classes of polymers and thus enable the identification and characterization of the multitude of possible structural transitions in adsorption processes under varied conditions. We study the phase changes by systematically modifying the energy scale associated with the adsorption strength between monomers and vertices of the hexagonal layer under the influence of thermal fluctuations. Advanced replica-exchange simulations [20–22] were performed and a variety of thermodynamic quantities and order parameters were analyzed statistically. Locations of extremal fluctuations of these quantities reveal qualitative changes in

arXiv:1912.00484v1 [cond-mat.soft] 1 Dec 2019

phase behavior and can be used for the localization and characterization as structural transitions.

The multiple transition lines thus identified are used to construct the hyperphase diagram of the system projected into the combined spaces of temperature and adsorption strength. The latter is an effective material parameter. This result is crucial for any future design of hybrid materials composed of soft polymer components and solid substrates with hexagonally shaped surface layer. As a consequence of the increasingly more specific adaptation process to the hexagonal surface structure at larger adhesion strengths, novel polymer phases occur. Intermolecular forces require the formation of local bridges between monomers located in the center of the hexagons under the constraint of limited elasticity of the bonds connecting adjacent monomers. The formation of characteristic highly oriented surface patterns of polymer conformations adsorbed at such substrates have not yet been investigated in much detail, although these substrate-induced stable polymer structures offer potential for nanoscale transport applications.

**Modeling and Simulation.** – In our generic model of the hybrid system, the flexible polymer is grafted with one end at a hexagonally patterned monolayer of attractive sites on an otherwise impenetrable substrate (see Fig. 1). We employ a recently introduced model for flexible polymers [23], in which the energy of a conformation, represented by the coordinate vector  $\mathbf{X} = (\mathbf{r}_1, \mathbf{r}_2, \dots, \mathbf{r}_N)$  for a linear chain with  $N$  monomers, is given by the contributions from nonbonded (NB) and bonded (B) pairs of monomers, respectively,

$$E_{\text{poly}}(\mathbf{X}) = \sum_{i < j} U_{\text{NB}}(r_{ij}) + \sum_i U_{\text{B}}(r_{ii+1}), \quad (1)$$

where  $r_{ij} = |\mathbf{r}_i - \mathbf{r}_j|$  is the distance between monomers  $i$  and  $j$ . Denoting the standard Lennard-Jones (LJ) potential with energy scale  $\epsilon$  and van der Waals radius  $\sigma$  by

$$U_{\text{LJ}}(r) = 4\epsilon[(\sigma/r)^{12} - (\sigma/r)^6], \quad (2)$$

pairs of nonbonded monomers interact via the potential

$$U_{\text{NB}}(r) = (U_{\text{LJ}}(r) - U_{\text{shift}})\Theta(r_c - r), \quad (3)$$

where  $\Theta(r)$  is the Heaviside step function. The cut-off distance is  $r_c = 2.5\sigma$  and  $U_{\text{shift}} = U_{\text{LJ}}(r_c)$  avoids a discontinuity of the potential at  $r = r_c$ . The minimum value of the potential is located at  $r_0 = 2^{1/6}\sigma$ . For bonded monomers, we choose a combination of the FENE (finitely extensible nonlinear elastic) [24–26] and the LJ potential in the following form:

$$U_{\text{B}}(r) = -\epsilon KR^2 \ln[1 - (r - r_0)^2/R^2]/2 + \eta[U_{\text{LJ}}(r) + \epsilon] - (U_{\text{shift}} + \epsilon). \quad (4)$$

The parameter  $\eta$  controls the symmetry and width of the potential [23]. In this study, we choose  $\eta = 1/10$ . The

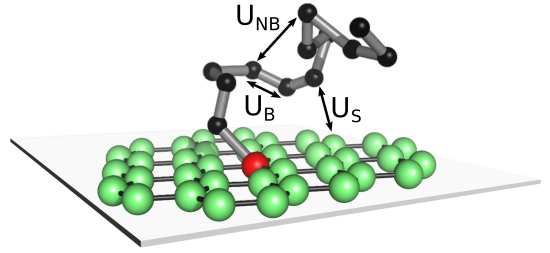


Fig. 1: Model of a flexible polymer with one end monomer (red) grafted onto a rigid hexagonal monolayer on an impenetrable substrate. The relevant potential energies for pairs of monomers and of monomers interacting with the attractive sites of the monolayer are also symbolized. Note that connections between monolayer sites are only shown as guides to the eyes to visually enhance its hexagonal structure and do not represent “bonds”.

other dimensionless parameters are set to  $K = 98/5$  and  $R = 3/7$  [23]. The minimum-potential distance, chosen to be  $r_0 \equiv 1$  in the simulations, sets the basic length scale. It represents the energetically optimal distance between the centers of two monomers (effective bond length). Energies are measured in units of the reference energy scale  $\epsilon \equiv 1$ . Hence, the temperature  $T$  scales in units of  $\epsilon/k_B$ , where  $k_B$  is the Boltzmann constant (also set to unity in our simulations).

Our model polymer with  $N = 55$  monomers is sufficiently long to identify the major structural effects without losing track of local and surface effects governing the different binding and folding mechanisms in the large parameter space covered by our structural analysis. The qualitative results do not depend significantly on the precise choice of the chain length. In this parameterization of the model, the ground-state structure of the free polymer is icosahedral [23]. However, for  $\epsilon_S \gg 0$  the interaction with the structurally incompatible hexagonal layer does not support quasicrystalline order in the polymer conformation. The formation of compact, adsorbed polymer conformations is governed by the recognition of the hexagonal structure of the monolayer and adaptation to it.

The energy associated with the interaction of the polymer with the laterally infinitely extended hexagonal monolayer can be written as

$$U_{\text{sub}}(\mathbf{X}) = \epsilon_S \sum_{i=2}^N U_{\text{S}}(\mathbf{r}_i). \quad (5)$$

The surface potential the  $i$ th monomer feels is given by

$$U_{\text{S}}(\mathbf{r}_i) = \sum_{a=1}^{\infty} U_{\text{NB}}(r_{ia}), \quad (6)$$

where  $a$  is a formal index for the vertices in the hexagonal lattice and  $r_{ia}$  is the distance between monomer  $i$  and vertex  $a$ . The same cut-off condition is used as in the potential for non-bonded monomers. The nearest-neighbor

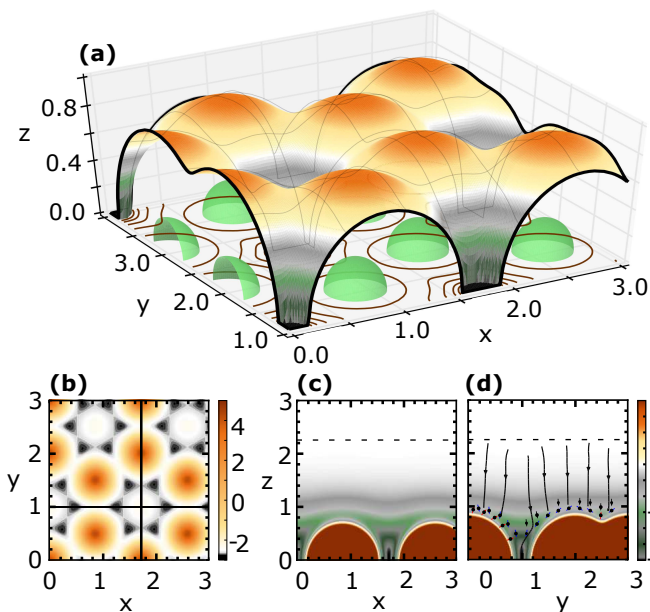


Fig. 2: Equipotential surface  $U_S(\mathbf{r}) \equiv 0$  (a) and three projections of the surface potential  $U_S(x, y, z)$  in the planes: (b)  $z = 0.81$ , (c)  $y = 1$ , and (d)  $x = \sqrt{3}$ . Note the saddle point at  $y = 2.5$  in (d) in addition to the stable potential minimum in the center of the hexagons.

distance between the attractive sites of the hexagonal layer is deliberately chosen so as to match the length scale  $r_0$  of the effective bonds between monomers.

The first monomer of the polymer chain is permanently attached to one vertex to prevent the polymer from escaping into the half-space above the substrate. Figure 2 shows the equipotential surface  $U_S(\mathbf{r}) \equiv 0$  as well as horizontal and vertical cross sections of the surface potential. The existence of the two minima is essential for the understanding of the structure formation mechanism of highly ordered and oriented adsorbed polymer conformations.

Eventually, the total energy of a polymer conformation  $\mathbf{X}$  is given by

$$E(\mathbf{X}) = E_{\text{poly}}(\mathbf{X}) + E_{\text{sub}}(\mathbf{X}). \quad (7)$$

Extensive parallel tempering replica-exchange [20–22] simulations of this model were performed to generate high-quality statistics for thermodynamic quantities needed for the analysis of the transition behavior in a large space of adsorption parameter values and temperatures. Typical simulations consisted of up to 128 simulation threads non-uniformly distributed in temperature space and chosen as to guarantee sufficient overlap of energy histograms necessary for an adequate exchange probability between simulation threads at neighboring temperatures. For the interpolation of results at intermediate temperatures, the multiple histogram reweighting procedure [27, 28] was employed.

**Statistical analysis.** – We analyzed a multitude of energetic and structural thermodynamic quantities and

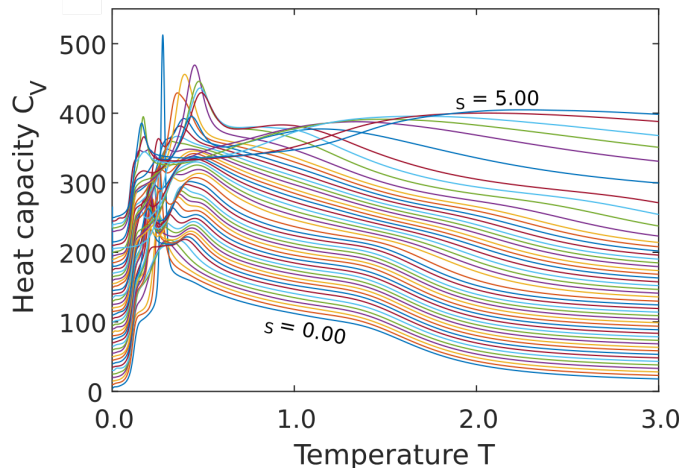


Fig. 3: Illustrative example for the transition complexity as indicated by features like peaks and “shoulders” (concave regions) in the heat-capacity curves  $C_V(T)$  for an array of the adsorption strength parameter  $\epsilon_S$  in the interval  $\epsilon_S \in [0.0, 5.0]$ . The curves are shifted vertically.

their fluctuations to identify pronounced features hinting to structural transitions in the system. The canonical statistical expectation value of a quantity  $O(\mathbf{X})$  is given by

$$\langle O \rangle(T) = \frac{1}{Z_{\text{can}}} \int \mathcal{D}\mathbf{X} O(\mathbf{X}) \exp[-\beta E(\mathbf{X})], \quad (8)$$

where

$$Z_{\text{can}} = \int \mathcal{D}\mathbf{X} \exp[-\beta E(\mathbf{X})] \quad (9)$$

is the canonical partition function at  $\beta = 1/k_B T$  and  $\mathcal{D}\mathbf{X}$  is the formal integral measure of all degrees of freedom in the space of polymer conformations  $\mathbf{X}$ . Thermal fluctuations are represented best by means of the response quantities (fluctuations)

$$\frac{d\langle O \rangle}{dT} = \frac{1}{k_B T^2} (\langle OE \rangle - \langle O \rangle \langle E \rangle). \quad (10)$$

Measurements of expectation values and fluctuations were performed in simulations for adsorption strength parameter values  $\epsilon_S \in [0.0, 5.0]$ .

Figure 3 shows the heat-capacity curves  $C_V(T) = d\langle E \rangle/dT$  for all simulated model parameter values as an example for the challenging task to consistently locate potential transition points. Other quantities such as the radius of gyration and components of the gyration tensor, end-to-end distance, numbers of contacts between pairs of monomers and lattice sites, and the center-of-mass location above the substrate have been used as more specific order parameters. Extremal fluctuations of these quantities help locate and characterize the various transitions.

**Structural hyperphase diagram.** – The major result of the detailed statistical analysis is the  $T$ - $\epsilon_S$  hyperphase diagram of the system, shown in Fig. 4 for  $\epsilon_S < 1.5$ .

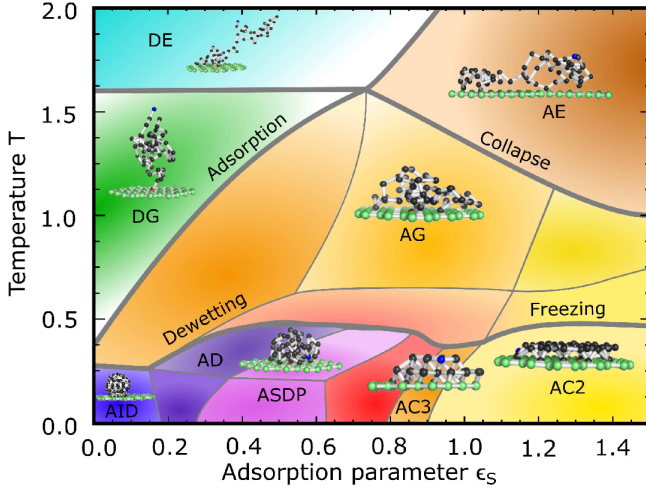


Fig. 4: Hyperphase diagram of a flexible polymer with 55 monomers interacting with a hexagonal monolayer. Representative polymer conformations are shown for major phases. See text for the description of the individual conformational phases. Since the studied system is finite, transition bands rather than lines indicate the uncertainty in locating transition points when analyzing multiple response quantities by canonical statistical analysis. It should also be noted that whereas the precise location of transition lines depends on the polymer chain length, the general, qualitative structure of the phase diagram does not significantly change for larger systems.

As expected, the polymer conformation is most compact at very low temperatures ( $T < 0.25$ ) and sufficiently small surface attraction ( $\epsilon_S < 0.2$ ). The structural phase of the polymer can be best characterized as “adsorbed icosahedral droplet” (AID). Even at  $\epsilon_S = 0$  the polymer is forced to reside in close proximity to the substrate despite the lack of attractive interaction. The tendency to maximize density while being grafted creates an effective spatial constraint. Increasing the temperature beyond the threshold  $T \approx 0.38$ , thermal fluctuations force the solid conformation to melt and an effective lift-off of the polymer is indicated by the structural order parameters we analyzed. In this phase polymer conformations are desorbed globules (DG). Upon further heating, entropic effects lead to the expected transition to desorbed expanded (DE) or random-coil structures. Adsorption of these polymer structures is enforced if the surface attraction of the substrate is large enough to overcompensate the effective (entropic) lifting force.

Like in the desorbed phases, lowering the temperature leads to the collapse of adsorbed expanded (AE) polymer structures, and adsorbed globular (AG) conformations form. The AG phase is a complex phase, which is divided in subphases dominated by globular droplets (below  $\epsilon_S < 0.6$ ), semispherical droplets ( $0.6 < \epsilon_S < 1.2$ ) and strictly double-layered disordered film-like structures ( $\epsilon_S > 1.2$ ), which represent the thinnest possible structures for this system (fluctuations in the direction perpen-

dicular to the substrate cease). Note the additional subphases around  $T \approx 0.5$  just above the dewetting/freezing transition lines, which are not present in phase diagrams of adsorption for systems with uniform substrates [12]. These additional subphases are caused by the adaptation of the flexible polymer to the hexagonal lattice structure of the monolayer. The surface layer of the polymer conformation takes on an ordered, organized shape, whereas the upper layers are still globular. Eventually, surface-layer structure formation is distinctly different at hexagonal sheets than near uniform substrates without inherent lattice structure [12]. Before we discuss these features in more detail, which, in fact, render globular and frozen double-layer phases indistinguishable for adsorption strengths  $\epsilon_S > 2.0$ , we first focus on the conformational properties of compact polymer structures for  $\epsilon_S < 1.5$ .

Similar to the heat-capacity curves shown in Fig. 3, fluctuation properties of all structural parameters analyzed in this study exhibit enormous complexity in the low-temperature regime associated with the structurally most compact phases for  $\epsilon_S < 1.5$ . This is due to the competing structural organization schemes in the surface layer of the polymer conformation in direct contact with the hexagonal sheet and the structure formation processes in upper, three-dimensionally extended, sections of compact conformations. Whereas the AID phase is unaffected by the sheet pattern, the adjacent phases of adsorbed droplets (AD) and adsorbed semi-spherical droplets (ASD) are split into two almost horizontal subphases. Similarly to the globular phase, dominant structures in the subphases differ in the arrangement of monomers in the layer closest to the hexagonal sheet.

At temperatures  $T > 0.25$ , the specific lattice structure of the sheet is not recognized and polymer crystallization proceeds as if the substrate was unstructured. However, at temperatures  $T < 0.25$ , reordering the monomers in accordance with the hexagonal sheet structure has small energetic advantages over entropic freedom and the appearance of the solid structures slightly changes. An intermediate phase, located roughly in the interval  $0.6 < \epsilon_S < 0.8$  represents an effective wetting/dewetting transition between most compact droplet and the adsorbed compact layered, crystalline phases with multiple (AC3) and eventually two (AC2) layers. Layering and adopting crystalline features thus occur once the surface adsorption strength is either competitive or dominates over inter-monomer attraction, i.e., for  $\epsilon_S > 0.8$ .

In these phases, monomers increasingly prefer contact with sheet vertices and intrude into the hexagonal sheet. However, since the hexagonal lattice is rigid, the distance between centers of adjacent hexagons is  $\sqrt{3}r_0 \approx 1.73r_0$  and the FENE potential prevents overstretching the bonds between bonded monomers beyond  $r_0 + R \approx 1.43r_0$ . Thus, at least three monomers are needed to fill centers of hexagons, with an intermediate monomer residing above the surface. The polymer must *build bridges* to achieve optimal packing. This is made possible by the condition-

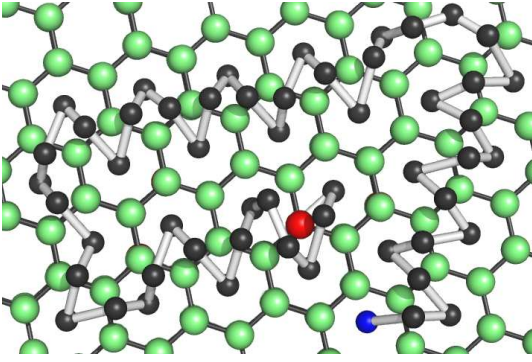


Fig. 5: Prominent example of a polymer conformation in the AZ nanorail phase. Since bonded monomers cannot reside in neighboring cells, an intermediate monomer is required to build a bridge across the hexagonal vertex bonds, forming stable segments of straight ridge lines (“rails”). The grafted monomer is colored in red, the terminal monomer of the chain in blue.

ally stable surface potential minima between vertices that are nearest neighbors in the hexagonal sheet [cf. Figs. 2(a, d)]. This also means that, for surface attraction strengths  $\epsilon_S > 1.0$ , the most compact film-like polymer conformation must have two layers (AC2). This is substantially different from the adsorption behavior at unstructured substrates [12]. Multiple-layer structures (in AC3) have a hexagonal closest packing (hcp) arrangement in striking contrast to polymer conformations at unstructured substrates which prefer forming face-centered cubic (fcc) structures. The hexagonal sheet truly imposes a structural constraint on the polymer, which leads to the formation of highly oriented, ordered conformations.

**Nanorail phase.** — The most amazing of these structures are formed if the vertex-monomer attraction exceeds but not entirely eclipses monomer-monomer attraction. The result are polymer conformations organized in a bundled zig-zag pattern reminiscent of planar helix bundles, but folded upward as the polymer cannot penetrate the substrate. A representative example is shown in Fig. 5. This arrangement and ordering is energetically preferential, because monomers located in the centers of neighboring hexagonal cells feel sufficient attraction to form strands in close proximity to each other. The upper layer is composed of parallel or specifically angled linear ridges that form a distinct pattern by themselves. Other structures can also form, but all have the distinctive adsorbed “zig-zag” (AZ) bridge pattern in common. The zig-zag pattern of the strands is stabilized by the attractive interaction of the monomers located in the ridge.

The AZ phase dominates at low temperatures for surface attraction strengths  $\epsilon_S > 2$ . Upon increasing temperature the only weakly bound monomers located in hexagon centers are entropically dissolved first, but the zig-zag pattern remains intact even at significantly higher temperatures. For example, at  $\epsilon_S = 3$ , the transition from the highly oriented AZ conformations to the phase of ad-

sorbed expanded zig-zag structures (AEZ) occurs at about  $T \approx 1.5$ . This means the hexagonal sheet is recognized by the polymer even at comparatively high temperatures until the polymer chain desorbs at about  $T \approx 6.0$ , where the majority of sheet-layer monomers are lifted off the hexagon centers for the gain of translational entropy at the expense of energetic benefits. It is worth noting that the ridges formed in the AZ phase can be straightened out by imposing energetic penalties for deviations from the optimal, alternating torsion angles dictated by the hexagonal lattice structure,  $60^\circ$  and  $120^\circ$ . The dominant bond angles we found for the straight segments are approximately  $50^\circ$  at the bridge foundation in the hexagon centers and about  $100^\circ$  at the crest of the bridge. These values cannot be explained easily by geometric considerations, because the bonds between monomers have to overstretch by more than 10% for large adsorption strengths. Under these conditions, the extremely stable ridge line is exactly linear and forms a “rail” along which molecular transport is possible.

**Summary and conclusions.** — Our study of the adsorption behavior of a flexible polymer at a hexagonally structured monolayer fixed on a solid substrate revealed a multitude of unique structural phases. Structure recognition and adaptation are mechanisms that lead to the formation of ordered and stable polymer conformations, which differ from adsorbed polymer structures at uniform substrates. A self-organized bridge-building mechanism enables the optimal coating of the hexagonal sheet and the formation of highly organized strands of monomers in parallel and angled arrangements. In actual applications, these polymer coats may help stabilize hexagonal sheets and nanotubes and add specific function. The high orientation of the polymer strands with their distinctive rail-like ridges [29, 30] enables directed molecular or vesicular transport on hexagonal substrates. Our results also motivate promising future studies such as nanoscale threading through penetrable sheets.

\*\*\*

B.L. acknowledges support by the Studienstiftung des deutschen Volkes (German Academic Scholarship Foundation). This work has been partially supported by the NSF under Grant No. DMR-1463241.

## REFERENCES

- [1] LIFSHITZ I. M., GROSBERG A. YU., AND KHOKHLOV A. R., *Rev. Mod. Phys.*, **50** (1978) 683.
- [2] DE GENNES P.-G., *Scaling Concepts in Polymer Physics* (Cornell University Press, Ithaca) 1979.
- [3] GRASSBERGER P., *Phys. Rev. E*, **56** (1997) 3682
- [4] WALES D. J. and DOYE J. P. K., *J. Phys. Chem. A*, **101** (1997) 5111.
- [5] DOYE J. P. K. and CALVO F., *J. Chem. Phys.*, **116** (2002) 8307.

- [6] SCHNABEL S., BACHMANN M., and JANKE W., *J. Chem. Phys.*, **131** (2009) 124904. (2018) 18835.
- [7] SCHNABEL S., SEATON D. T., LANDAU D. P., and BACHMANN M., *Phys. Rev. E*, **84** (2011) 011127.
- [8] BACHMANN M., *Thermodynamics and Statistical Mechanics of Macromolecular Systems* (Cambridge University Press, Cambridge) 2014.
- [9] VRBOVÁ T. and WHITTINGTON S. G., *J. Phys. A: Math. Gen.*, **29** (1996) 6253.
- [10] KRAWCZYK J., PRELLBERG T., OWCZAREK A. L., and RECHNITZER A., *Europhys. Lett.*, **70** (2005) 726.
- [11] IVANOV V. A., MARTEMYANOVA J. A., MÜLLER M., PAUL W., and BINDER K., *J. Phys. Chem. B*, **113** (2009) 3653.
- [12] MÖDDEL M., BACHMANN M., and JANKE W., *J. Phys. Chem. B*, **113** (2009) 3314.
- [13] MILCHEV A. and BINDER K., *J. Chem. Phys.*, **117** (2002) 6852.
- [14] GUREVITCH I. and SREBNIK S., *Chem. Phys. Lett.*, **444** (2007) 96.
- [15] VOGEL T. and BACHMANN M., *Phys. Rev. Lett.*, **104** (2010) 198302.
- [16] HU K., KULKARNI D. D., CHOI I., and TSUKRUK V. V., *Prog. Polym. Sci.*, **39** (2014) 1934.
- [17] SU Y., HAN H.-L., CAI Q., WU Q., XIE M., CHEN D., GENG B., ZHANG Y., WANG F., SHEN Y. R., and TIAN C., *Nano Lett.*, **15** (2015) 6501.
- [18] GEIM A. K. and NOVOSELOV K. S., *Nature Mat.*, **6** (2007) 183.
- [19] JORIO A., DRESSELHAUS G., and DRESSELHAUS M. S. (Editors), *Carbon Nanotubes: Advanced Topics in the Synthesis, Structure, Properties, and Applications*, Topics in Applied Physics, Vol. **111** (Springer, Berlin, Heidelberg) 2008.
- [20] SWENDSEN R. H. and WANG J.-S., *Phys. Rev. Lett.*, **57** (1986) 2607.
- [21] HUKUSHIMA K., TAKAYAMA H., and NEMOTO K., *Int. J. Mod. Phys. C*, **7** (1996) 337.
- [22] GEYER C. J., *Computing Science and Statistics, Proceedings of the 23rd Symposium on the Interface*, edited by KERAMIDAS E. M. (Interface Foundation, Fairfax Station) 1991, p. 156.
- [23] QI K., LIEWEHR B., KOCI T., PATTANASIRI B., WILLIAMS M. J., and BACHMANN M., *J. Chem. Phys.*, **150** (2019) 054904.
- [24] BIRD R. B., CURTISS C. F., ARMSTRONG R. C., and HASSAGER O., *Dynamics of Polymeric Liquids*, 2nd edition, (Wiley, New York) 1987.
- [25] KREMER K. and GREST G. S., *J. Chem. Phys.*, **92** (1990) 5057.
- [26] MILCHEV A., BHATTACHARAYA A., and BINDER K., *Macromolecules*, **34** (2001) 1881.
- [27] FERRENBERG A. M. and SWENDSEN R. H., *Phys. Rev. Lett.*, **63** (1989) 1195.
- [28] KUMAR S., BOUZIDA D., SWENDSEN R. H., KOLLMAN P. A., and ROSENBERG J. M., *J. Comput. Chem.*, **13** (1992) 1011.
- [29] TAMARU S. I., IKEDA M., SHIMIDZU Y., MATSUMOTO S., TAKEUCHI S., and HAMACHI I., *Nature Commun.*, **1** (2010) 20.
- [30] VASIĆ B., STANKOVIĆ I., MATKOVIĆ A., KRATZER M., GANSER C., GAJIĆ R., and TEICHERT C., *Nanoscale*, **10**